Cancer & Metabolism

RESEARCH Open Access

Exploratory profiling of metabolites in cerebrospinal fluid using a commercially available targeted LC-MS based metabolomics kit to discriminate leptomeningeal metastasis

Soojin Jang[1], Ho-Shin Gwak[2,5*], Kyue-Yim Lee[2], Jun Hwa Lee[3], Kyung-Hee Kim[3], Jong Heon Kim[4], Jong Bae Park[4], Sang Hoon Shin[5], Heon Yoo[5], Yun-Sik Dho[5], Kyu-Chang Wang[5] and Byong Chul Yoo[6]

Abstract

Background Leptomeningeal metastasis (LM) is a devastating complication of cancer that is difficult to treat. Thus, early diagnosis is essential for LM patients. However, cerebrospinal fluid (CSF) cytology has low sensitivity, and imaging approaches are ineffective. We explored targeted CSF metabolic profiling to discriminate among LM and other conditions affecting the central nervous system (CNS).

Methods We quantitatively measured amino acids, biogenic amines, hexoses, acylcarnitines (AC), cholesteryl esters (CE), glycerides, phosphatidylcholines (PC), lysophosphatidylcholines (LPC), sphingomyelins (SM), and ceramides (Cer) in 117 CSF samples from various groups of healthy controls (HC, $n=10$), patients with LM (LM, $n=47$), parenchymal brain tumor (PBT, $n=45$), and inflammatory disease (ID, $n=13$) with internal standards using the Absolute IDQ- p400® targeted mass spectrometry kit. Metabolites detected in > 90% of samples or showing a difference in proportional level between groups ≥ 75% were used in logistic regression models when there was no single metabolite with AUC = 1 for the groups of comparison.

Results PC and SM had higher levels in LM than in PBT or HC, whereas LPC had lower level in PBT than the other groups. Glycerides and Cer levels were higher in PBT and LM than in HC. Long-chain AC level in PBT was lower than in LM or HC. A regression model including Ala, PC (42:7), PC (30:3), PC (37:0), and Tyr achieved complete discrimination (AUC = 1.0) between LM and HC. In comparison of PBT and HC, twenty-six individual metabolites allowed complete discrimination between two groups, and between ID and HC fourty-six individual lipid metabolites allowed complete discrimination. Twenty-one individual metabolites (18 ACs and 3 PCs) allowed complete discrimination between LM and PBT.

Conclusions Using a commercial targeted liquid chromatography-mass spectrometry (LC-MS) metabolomics kit, we were able to differentiate LM from HC and PBT. Most of the discriminative metabolites among different diseases were lipid metabolites, for which their CNS distribution and quantification in different cell types are largely unknown,

*Correspondence:
Ho-Shin Gwak
nsghs@ncc.re.kr

Full list of author information is available at the end of the article

whereas amino acids, biogenic amines, and hexoses failed to show significant differences. Future validation studies with larger, controlled cohorts should be performed, and hopefully, the kit may expand its metabolite coverage for unique cancer cell glucose metabolism.

Keywords Cerebrospinal fluid, Metabolome, Leptomeningeal metastasis, Profile, Diagnosis

Introduction

Cerebrospinal fluid (CSF) bathes the central nervous system (CNS), transporting neurotransmitters and other bioactive substances such as hormones and active/passive secretory compounds produced by brain cells [1]. Researchers analyze CSF to detect biomarkers of diseases including Alzheimer's dementia, Parkinson's disease, demyelinating diseases, and tumors [2, 3]. Candidate biomarkers of CSF have been diverse but are often specific for a certain disease including proteins such as amyloid β and tau in Alzheimer's dementia, tumor-specific antigens for germ cell tumors, and microRNAs, cell-free DNA, or other molecules such as cytokines for CNS tumors [2–6]. Among these, the metabolic profile provides a quantifiable readout of biochemical states ranging from normal physiology to diverse pathophysiologies, which may not be apparent in gene expression analyses [7].

Metabolites can be detected as low-mass ions (LMIs) in non-targeted mass spectrometry (MS) or as the unique resonance of proton in nuclear magnetic resonance spectroscopy in a semi-quantitative manner for metabolomics analysis. The resulting metabolomic profiles of various biofluids from cancer patients reflect the unique characteristics of the tumor microenvironment, providing a method for early diagnosis and identification of distinctive signatures for various cancer types [8–13]. However, non-targeted MS should be re-evaluated with appropriate standard materials by a quantitative method (i.e. targeted liquid chromatography-mass spectrometry (LC-MS)), and all associated metabolites should be evaluated together for discriminative profiling according to metabolic changes. In this context, a commercially available targeted quantitative MS kit that measures hundreds of metabolites from hundreds of samples together would be helpful to overcome the limitations of non-targeted or semi-quantitative metabolomics and to gather data from many samples with minimal intra-/inter-laboratory bias.

Leptomeningeal metastasis (LM) is a terminal stage of cancer that rapidly deteriorates patient performance. Overall survival of patients with LM is approximately 6–8 weeks after symptom presentation if not properly treated [14]. Even current treatment options of intra-CSF chemotherapy and radiation therapy result in marginal survival benefit without discernible symptom improvement or definite cure [15]. Thus, early diagnosis of LM in high risk patients and an understanding of the relevant pathophysiology to develop targeted therapy are necessary to improve outcomes of patients with LM; however, the current diagnostic tool of CSF cytology has low sensitivity (50–60%) due to a paucity of floating cancer cells, and gadolinium-enhanced magnetic resonance imaging (MRI) is neither capable of early detection nor pathognomonic for LM because of varying non-specific leptomeningeal enhancement [16–18].

Previously, we used liquid chromatography-tandem mass spectrometry (LC-MS/MS) to analyze metabolic profiles of CSF from a relatively large number of patients ($n = 196$) [19]. Using principal component analysis (PCA) based discriminant analysis, we identified 1,440 discriminative LMIs that could differentiate LM from parenchymal brain tumors (PBT), including brain metastasis (BM) and primary brain tumors (BT), which have a high risk of developing LM. Although we are still in the process of validating this LMI profile with targeted MS, it has been time-consuming to identify candidate LMIs in MS/MS results, and it has also been difficult to have appropriate internal standards for quantification.

In this study, we explored the metabolomic profiles of CSF from healthy controls (HC) and patients with LM or PBT using the commercially available Absolute IDQ-p400® targeted metabolomics kit (Biocrates Life Science AG) for high-resolution mass spectrometry (HRMS). This kit enables quantification of 408 metabolites including amino acids, biogenic amines, hexose, and polar/non-polar lipids. We evaluated the levels of different metabolites and metabolite classes for differences due to cancer cell activity and characteristics of the tumor microenvironment. Furthermore, we identified specific metabolite profiles that were able to discriminate among LM, PBT, and inflammatory disease (ID). We also explored whether comparative profiling of CSF metabolites could discriminate between different CNS tumor characteristics (e.g., glial vs. non-glial) and other clinical factors.

Materials and methods

CSF archives

CSF samples were obtained after Institutional Review Board approval (NCC2014-0135) from patients who had already submitted informed consent. CSF samples were mostly obtained via lumbar puncture for CSF cytology examination in cases of LM, BM, and BT, or for diagnostic evaluation in ID cases. Additional CSF samples were collected from the cisternal/subarachnoid space during craniotomy for tumor removal: BM and BT; or clipping of an unruptured aneurysm: HC. All LM patients had both

a cytological diagnosis of LM and a positive neuroimaging study (gadolinium-enhanced brain MRI/whole-spine MRI) [16]. CSF samples were centrifuged (2,000×*g* for 20 min, within 1 h of collection) at room temperature to pellet cells, and the supernatant was aliquoted. A 50-μL sample of each supernatant for MS analysis was instantly kept in freezer (−80 °C) until metabolite extraction. The remaining samples were centrifuged again at 10,000×*g* for 30 min and kept frozen at − 80 °C for further study.

Targeted CSF metabolome measurement

A targeted metabolomic analysis was performed using the Absolute IDQ-p400® kit (Biocrates Life Science AG, Innsbruck, Austria), a commercially available assay that was originally developed for plasma and covers 408 metabolites from 11 metabolite classes. The largest metabolite class covered was phosphatidylcholines (PC, $n = 196$), followed by acylcarnitines (AC, $n = 55$), triglycerides (TG, $n = 42$), sphingomyelins (SM, $n = 31$), lysophosphatidylcholines (LPC, $n = 24$), amino acids ($n = 21$), biogenic amines ($n = 21$), diglycerides (DG, $n = 18$), cholesteryl esters (CE, $n = 14$), ceramides (Cer, $n = 9$), and monosaccharides ($n = 1$), which included the total of hexoses. The LC-HRMS method was used to quantify amino acids and biogenic amines, while flow injection analysis (FIA) HRMS was used to assess AC, CE, glycerophospholipids (e.g., PC and LPC), glycerides (e.g., DG and TG), sphingolipids (e.g., SM and Cer), and hexoses.

The kit provided quantitative measurements for amino acids, biogenic amines, and hexoses with internal standards provided by the manufacturer [20]. The rest of the metabolites were measured semi-quantitatively, using standards with similar chemical properties as the targets (a version of one-point calibration).

Metabolite extraction and preparation

Briefly, frozen CSF samples were placed on ice until completely thawed and then centrifuged at 2,750×*g* for 5 min at 4 °C. According to recommendations from the kit manufacturer, 30 μL aliquots of internal standard mix, CSF sample, blank, zero sample, and kit quality control materials were each added directly onto a 96-well plate and dried under nitrogen flow. The dried samples were derivatized using 5% phenylisothiocyanate, incubated for 25 min, and dried under nitrogen flow. After drying, 300 μL extraction solvent (5 mM ammonium acetate in methanol) was added and shaken for 30 min at 450 rpm. The contents of the wells were filtered into a lower plate by centrifugation at 500×*g* for 2 min. The extracted samples were diluted for subsequent LC-MS/MS and FIA-MS/MS analysis.

LC-MS/MS and FIA-MS/MS analyses

The extracted samples were analyzed using a Q Exactive™ Plus Hybrid Quadrupole-Orbitrap mass spectrometer (Thermo Fisher Scientific) coupled with a Vanquish Flex UHPLC system (Thermo Fisher Scientific). For LC-MS/MS analysis, samples were loaded onto a trap column (SecurityGuard™ ULTRA Cartridges UHPLC C18, 2.1 mm) and gradient separated on an analytical column (Biocrates) with solvent B (0.2% formic acid in acetonitrile) concentration from 0 to 12% for 1.25 min, from 12 to 17.5% for 1.2 min, from 17.5 to 50% for 1.3 min, and from 50 to 95% for 0.5 min. The eluted metabolites were sprayed onto a Heat Electrospray Ionization (HESI-II) source with electrospray voltage of 3.0 kV. The Q Exactive Orbitrap mass analyzer was operated in either full MS mode or parallel reaction monitoring (PRM) mode. Full MS scans were acquired over the range m/z 55–800 with mass resolution of 70,000 (at m/z 200). PRM scans were fragmented in the higher-energy collisional dissociation collision cell with normalized collision energy of 30, and tandem mass spectra were acquired in the Orbitrap mass analyzer with a mass resolution of 35,000 at m/z 200. For FIA-MS/MS analysis, samples were sprayed onto an HESI-II source with electrospray voltage of 2.5 kV. The Q Exactive Orbitrap mass analyzer was operated in full MS mode. Full MS scans were acquired over eight different m/z ranges according to the manufacturer's instruction, with mass resolution of 70,000 (at m/z 200). The acquired spectra were analyzed using Xcalibur™ (Thermo Fisher Scientific) and MetIDQ™ (Biocrates) software.

CSF metabolite profiling according to patient groups

Candidate metabolites

As the goal of this study was to set a discriminative profile based on standardized targeted MS, we used metabolites that were measured in > 90% of all CSF samples as candidate metabolites for discrimination. However, if a metabolite that was measured in less than 90% of all CSF samples was present in proportions that differed by at least 75% between comparison groups (e.g., PC (44:7) was detected in 10 out of 49 LM samples (80%) but in none of the HC samples), we assumed that the metabolite was uniquely present in one group and included it as a candidate metabolite, regardless of its overall detection rate across all CSF samples.

Select discriminative metabolites and compose a discriminative model

To identify the candidate metabolites with the greatest power to discriminate among the patient groups, we selected 'discriminative metabolites' that showed an AUC ≥ 0.75 for a given comparison between patient groups. To make a discriminative model, we used logistic regression when there was no metabolite with AUC = 1

for a given comparison. The model was started using the two individual metabolites with the top two AUCs for the comparison of interest and then iteratively updated by adding the metabolite with the next highest AUC, until the model achieved an AUC = 1 or there were no more individual metabolites with an AUC ≥ 0.75.

Statistical analyses

R for Windows (v4.3.2) was used for all statistical analyses. The PCA was done using the FactoMineR (Sebastien Le, Julie Josse, Francois Husson (2008). FactoMineR: An R Package for Multivariate Analysis. Journal of Statistical Software, 25(1), 1–18. https://doi.org/10.18637/jss.v025.i01) and factoextra (Kassambara A, Mundt F (2020). _factoextra: Extract and Visualize the Results of Multivariate Data Analyses. R package version 1.0.7, <https://CRAN.R-project.org/package=factoextra>.) packages. The heatmap was drawn using the pheatmap (Kolde R (2019). _pheatmap: Pretty Heatmaps_. R package version 1.0.12, <https://CRAN.R-project.org/package=pheatmap>.) package.

Quantitative values of metabolite concentrations in two groups were compared using t-test or rank sum test, depending on the results of a Shapiro–Wilk test for normality. A two-tailed p value < 0.05 was considered statistically significant after false discovery rate correction for multiple comparisons.

Results

Clinical characteristics of the patients

A total of 117 CSF samples were obtained from 49 patients with LM and 68 control patients, including HC with no parenchymal brain disease but unruptured aneurysm. The demographic characteristics of the participants are summarized in Supplementary Table 1. The primary cancer in all patients with LM was either non-small-cell lung carcinoma or breast cancer, and those two primary cancers each accounted for six of the 15 cases of BM. In this context, females were more common than males in our sample due to the prevalence of breast cancer cases. As we did not restrict patient age in our sample, the patients' ages ranged from 1 year to 81 years (median, 48 years). Patients with BT were intentionally selected to include 10 individuals from each of three groups: those with extra-axial benign tumors, glial tumors, and non-glial malignant brain tumors. Patients with ID included five with bacterial CSF infection and eight with demyelinating disease, of whom five had multiple sclerosis and three had transverse myelitis.

The CSF sampling sites included the lumbar region with 53 samples, the ventricular region with 50 samples, and the cisternal region with 14 samples, selected according to the sampling conditions described in the Methods section (Supplementary Table 2).

Proportions of detected metabolites among the CSF samples

The levels of each measured metabolite in CSF samples are listed in Supplementary Table 2. Overall, 201 metabolites (50%) were detected in > 90% of the samples, with 136 metabolites (34%) detected in every sample. In contrast, 102 metabolites (26%) were found in ≤ 50% of the samples, and 35 metabolites (8.7%) were present in ≤ 10% of the samples (Fig. 1A). The levels of different metabolite classes were detected in varying proportions across the total samples, except for hexoses, which were detected in all samples (Fig. 1B). Of the 21 amino acids measured, 19 were detected in all the samples, while Asp and Ile were each undetected in 9 samples (7.7%). Among the eight metabolite classes, biogenic amines were detected in the smallest proportion of samples. Specifically, 10 out of 21 biogenic amines, including dopamine, histamine, and serotonin, appeared in < 10% of the samples. In contrast, creatinine, SDMA, t4-OH-Pro, and taurine were each detected in all samples. Spermidine was absent in all HC samples but detected in 17 of 49 LM samples, 15 of 45 PBT samples, and 6 of 13 ID samples.

Determining the proportional levels of different lipids was complicated because of the various lengths and double bonds of fatty acid chains within the same lipid subclasses (hereafter referred to as variants). Among the different subclasses of lipids, Cer were detected in the highest proportion of samples, with all variants present in > 90% of the samples, and 5/9 variants detected in every sample. By contrast, SM were detected in a relatively low proportion of samples, with only 2/31 (6.5%) variants detected in > 90% of the samples, and 20/31 (65%) variants detected in < 50% of the samples. Following Cer, AC were the next most common subclass of lipid metabolites among the samples, with 43/55 (78%) AC variants detected in > 90% of the samples and 41 variants (75%) detected in all the samples. Within the CE, DG, and TG subclasses of neutral lipids, 5/14 (36%), 11/18 (61%), and 21/42 (50%) variants were detected in > 90% of the samples, respectively. Of total 170 lipid subclass variants detected in the analysis, PC had the greatest number of tested variants among the metabolite subclasses. Eighty-two (48%) PC variants were detected in > 90% of the samples, whereas 30 (18%) PC variants were detected in < 50% of the samples. Only five (2.9%) PC variants were detected in < 10% of the samples. Among the glycerophospholipids, LPC were detected in the lowest proportions of samples, as none of the variants were detected in > 90% of the samples. Twenty out of 23 (87%) LPC variants were detected in < 50% of the samples, and 11 (48%) LPC variants were detected in < 10% of the samples.

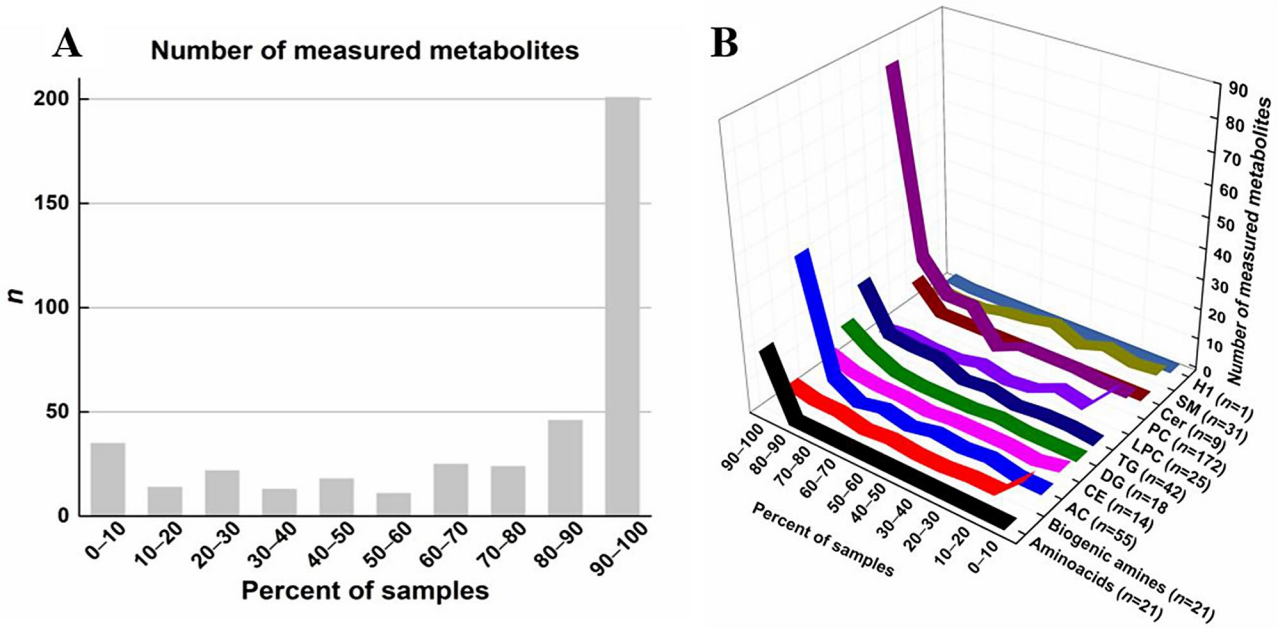

Fig. 1 Measured metabolites in cerebrospinal fluid. **A** The numbers of metabolites detected in different proportions of samples. **B** The numbers of metabolites in each metabolite class detected in different proportions of samples. Notes: AC, acylcarnitines; CE, cholesteryl esters; Cer, ceramides; DG, diglycerides; H1, hexoses; LPC, lysophosphatidylcholines; PC, phosphatidylcholines; SM, sphingomyelins; TG, triglycerides

Differential metabolites levels among patient groups

To explore differences in metabolite levels among the patient groups, we performed PCA and supervised hierarchical clustering analysis (HCA) with 201 metabolites that were detected in > 90% of the CSF samples.

In the PCA plot, HC formed a relatively homogeneous and distinct cluster, while the other patient groups mostly overlapped, with LM showing the widest distribution (Fig. 2A). In the supervised HCA, the metabolite profiles of the two PBT subgroups (BM and BT) showed high similarity to each other (Fig. 2B). The metabolite profile of ID was also relatively similar to those of the two PBT subgroups, whereas the metabolite profile of LM was divided into two patterns: one (59%) similar to that of HC and the other (41%) similar to those of PBT and ID.

While the volcano plot reveals some metabolites with differential levels between LM and NonLM groups, the lack of distinct patterns or standout features limits the identification of specific significant metabolites (Supplementary Fig. 1).

Differential level of metabolite classes among PBT, LM, and HC

To gain a more in-depth understanding of different metabolic activities among PBT, LM, and HC, we averaged the measured metabolite levels in each group according to metabolite classes (Supplementary Table 3). Amino acids and biogenic amines levels showed no significant difference among the patient groups (Supplementary Fig. 2). Hexose levels were affected by each patient's history of intravenous infusion and steroid use (Supplementary Table 4). Among the lipids, CE showed higher levels in LM than in PBT or HC, but the differences failed to reach statistical significance (Fig. 3A). Other non-polar glycerides (DG and TG) showed significantly higher levels in PBT and LM than in HC (Fig. 3B). Among the glycerophospholipids, PC levels followed a pattern similar to that of CE, with significantly higher levels in LM than in PBT or HC, whereas LPC levels were significantly lower in PBT compared to LM or HC (Fig. 3C). Among the sphingolipids, SM had higher levels in LM than in PBT or HC, similar to the pattern of PC level, whereas Cer showed a pattern similar to that of the glycerides, with higher levels in PBT and LM than in HC (Fig. 3D).

For the ACs, we calculated average levels separately according to the fatty acid chain length, based on a previous report indicating that long-chain ACs are transporters involved in mitochondrial β-oxidation [21]. Total AC and short/medium-chain AC levels were apparently higher in LM than in PBT or HC, although the difference failed to reach statistical significance, whereas long-chain AC level was significantly lower in PBT than in LM or HC (Fig. 3E). To determine whether the low level of long-chain AC in PBT was due to decreased production or increased consumption, we calculated the enzymatic activities of carnitine palmitoyltransferase 1 [CPT1; (AC C16 + AC C18) / carnitine], which enables AC transport from the cytosol to the mitochondria, and carnitine palmitoyltransferase 2 [CPT2; (AC C16 + AC C18:1) / AC C2], which converts mitochondrial AC into Acyl-CoA

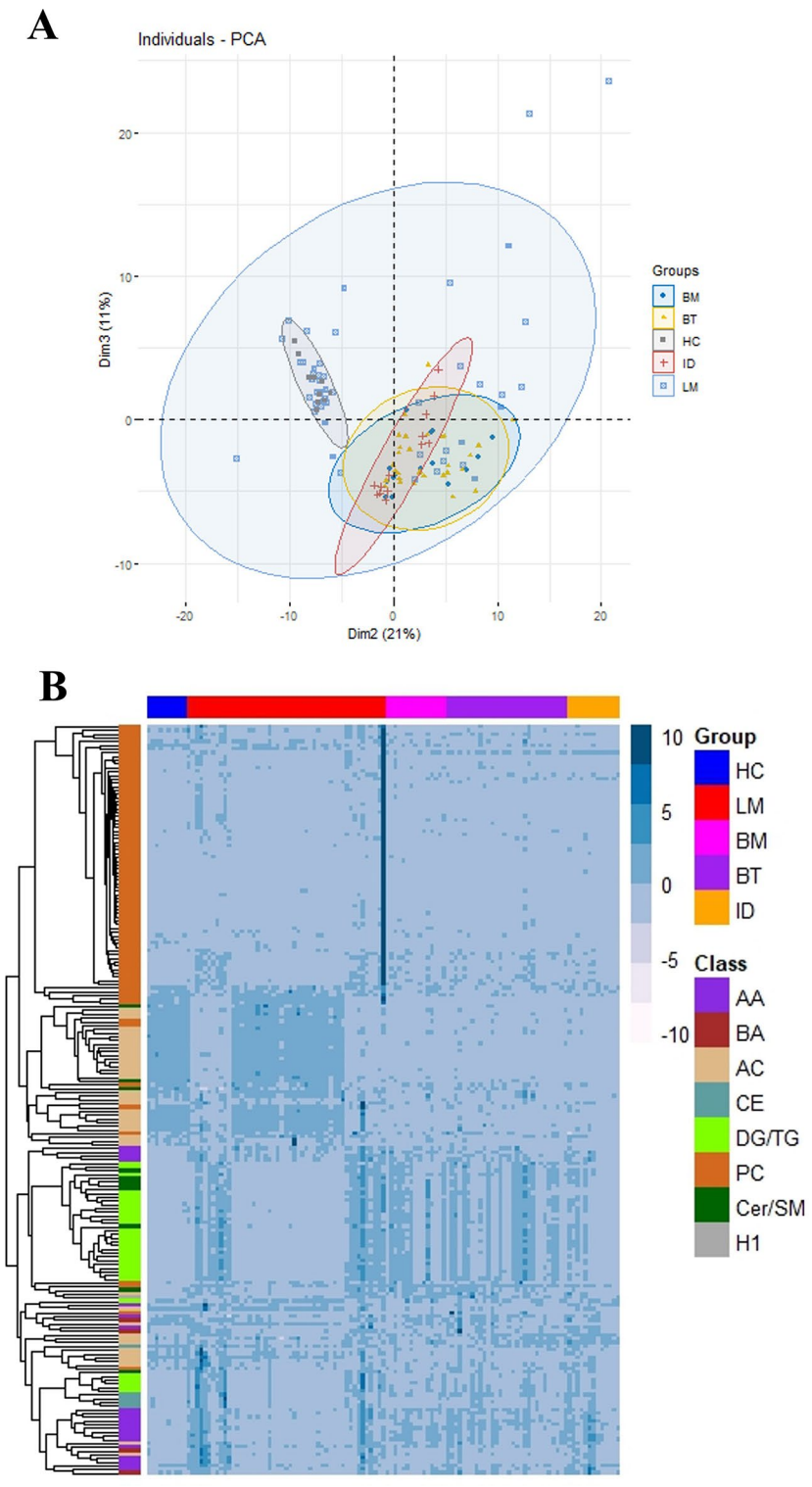

Fig. 2 Differentially detected metabolites among patient groups. **A** Principal component analysis plot showing a relatively discrete HC cluster and a widely distributed LM cluster. **B** Supervised clustering (LM vs. HC) heatmap of 117 samples with CSF metabolomes was generated using 201 metabolites measured > 90% of samples. Notes: BM, brain metastasis; BT, brain tumor; HC, healthy control; ID, inflammatory disease; LM, leptomeningeal metastasis; AA, aminoacids; BA, biogenic amines; AC, acylcarnitines; CE, cholesteryl esters; DG, diglycerides; TG, triglycerides; PC, phosphatidylcholines; Cer, ceramides; SM, sphingomyelins; H1, hexoses

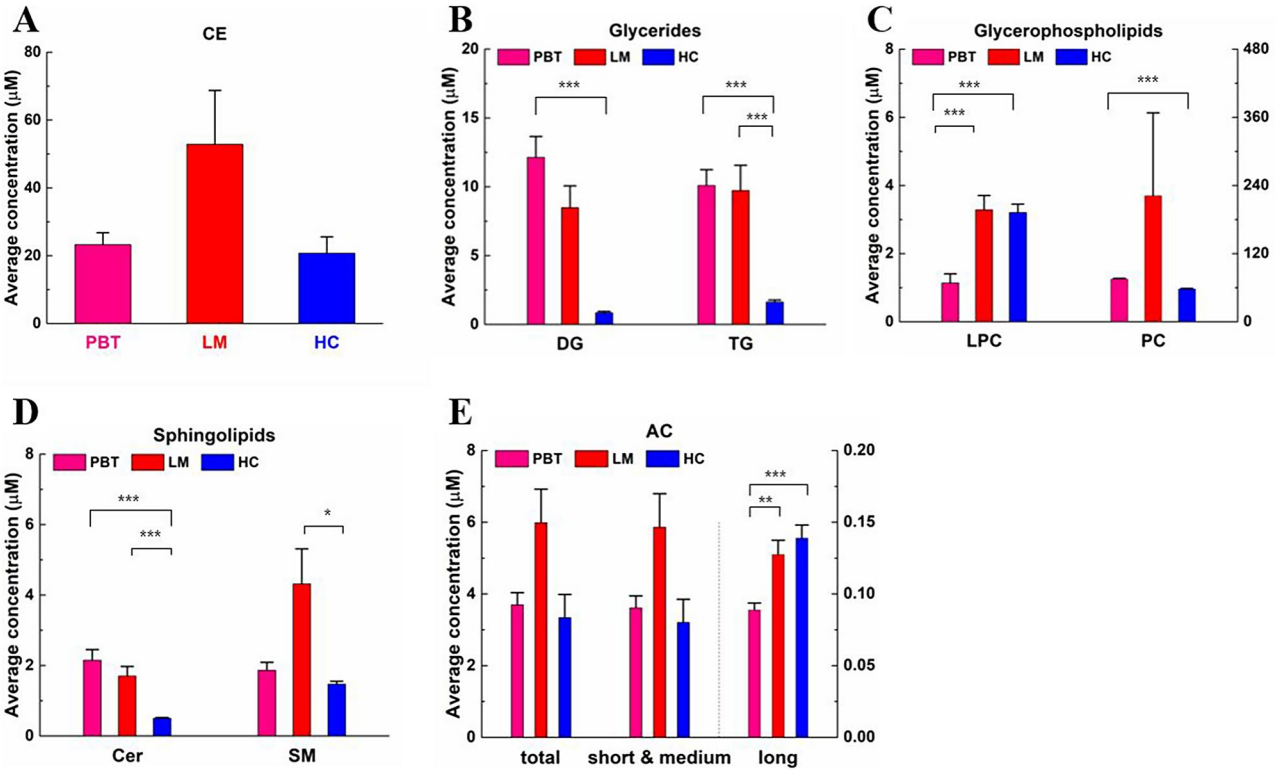

Fig. 3 Levels of each lipid metabolite class according to tumor status. **A** Cholesteryl esters. **B** Glycerides. **C** Glycerophospholipids. **D** Sphingolipids. **E** Acylcarnitines. Error bars represent the mean standard error. (* $0.01 < p < 0.05$; ** $0.001 < p < 0.01$; *** $p < 0.001$). Notes: HC, healthy control; LM, leptomeningeal metastasis; PBT, parenchymal brain tumor

to enable the return of carnitine to the cytosol [22]. The enzymatic activity of CPT1 was significantly lower in PBT than in LM or HC (Supplementary Fig. 2). Although the enzymatic activity of CPT2 showed a similar pattern, only the difference between HC and PBT was significant. Therefore, we tentatively concluded that the lower level of long-chain AC in PBT compared with LM and HC resulted from low efficacy of β-oxidation due to decreased CPT1 and CPT2 enzymatic activities.

Discriminative metabolomic profiles

To determine if the CSF metabolomic profiles have diagnostic value, we extracted candidate metabolites and composed discriminative metabolite profiles that achieved AUC = 1.0.

LM versus HC

To discriminate between LM and HC, 179 metabolites met the criteria of candidate metabolites, defined as those either detected in > 90% of all CSF samples or with a proportion difference of ≥ 75% between two groups. Among these, 28 metabolites were identified as discriminative (AUC > 0.75; Supplementary Table 5), comprising 9 AC, 8 amino acids, 5 PC, 3 glycerides, 2 biogenic amines, and 1 Cer. All AC levels were higher in HC than in LM, while 7 out of 8 amino acids had higher levels in LM than in HC. The top five metabolites—Ala, PC(42:7), PC(30:3), PC(37:0), and Tyr—with individual AUCs of 0.87 to 0.92, achieved an AUC of 1.0 collectively in a logistic regression model (Fig. 4).

PBT and ID versus HC

As we assumed that LM likely shares characteristics of both CNS tumors and inflammation in terms of pial attachment and disruption, we first identified metabolites that could be used to discriminate between HC and either PBT or ID (Supplementary Table 6). Then, we identified metabolites to discriminate separately between PBT and HC and between ID and HC.

Out of 241 candidate metabolites for discriminating between PBT and HC, we identified 178 discriminative metabolites, including 26 metabolites showing both 100% sensitivity and 100% specificity (AUC = 1.0). All 26 discriminative metabolites were lipids, and among these, all 14 AC and 1 LPC had higher levels in HC than in PBT, whereas all 11 PC had higher levels in PBT than in HC.

Among 223 candidate metabolites for discriminating between ID and HC, 153 were identified as discriminative, with 46 showing an AUC of 1.0. Except for putrescine, all of these were lipids. Of the 46 molecules with an AUC of 1.0, all 21 AC, 6 out of 20 PC, both Cer, and LPC had higher levels in HC than in ID, whereas 14 out of 20

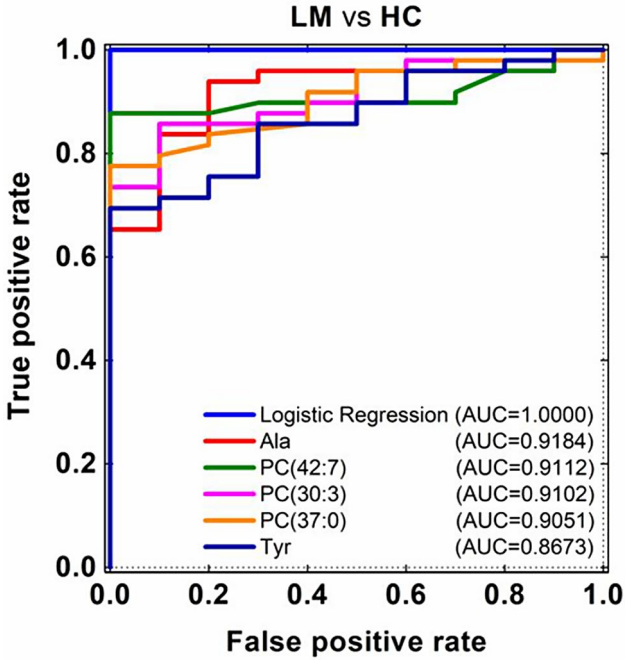

Fig. 4 Receiver operating curves of the top five discriminative metabolites for leptomeningeal metastasis and healthy controls. The area under the curve (AUC) for a logistic regression model included all five metabolites is also shown. Notes: HC, healthy control; LM, leptomeningeal metastasis

PC, DG, and putrescine had higher levels in ID than in HC.

LM versus PBT

As about 75% of LM stems from pre-existing BM or brain tumor [23], it is valuable to know if metabolite profiles can discriminate between LM and PBT, which has a high risk of developing LM. Among 208 metabolites that met the criteria of candidate metabolites, 44 were discriminative (Supplementary Table 7). The discriminative metabolites with the top 21 AUC values (ranging from 0.83 to 0.94), all of which were AC or PC, together achieved an AUC of 1.0 in a logistic regression model. Among these, all 18 AC, PC(38:1), and PC(36:0) had higher levels in LM than in PBT, with PC(44:3) being the exception.

Characteristics of LM discriminative metabolites compared with PBT and ID discriminative metabolites

We tentatively defined the metabolites that were discriminative between PBT and HC to be 'tumorous,' between ID and HC to be 'inflammatory,' and between LM and PBT to be 'LM diagnostic.' Then, we examined the similarities and differences among these metabolite sets (Supplementary Table 8).

127 metabolites were shared between the 'tumorous' and 'inflammatory' sets, accounting for 71% of all 'tumorous' metabolites and 83% of all 'inflammatory' metabolites (Fig. 5A). These included 57 glycerophospholipids (45%), 36 AC (28%), 12 glycerides (9.4%), 11 amino acids (8.7%), 7 sphingolipids (5.5%), 2 biogenic amines, 1 cholesterol ester, and hexose. All 127 metabolites had the same qualitative pattern of increased or decreased levels in both PBT and ID relative to HC. For example, Thr level was higher in both PBT and ID than in HC (Fig. 5B), whereas AC(4: 0) level was vice versa (Fig. 5C). These findings suggested that many of the 'tumorous' metabolites shared production/consumption pathways with inflammatory responses. We next examined the differences between metabolites that were unique to the 'tumorous' set or the 'inflammatory' set. Among the 51 metabolites that belonged to the 'tumorous' set and not the 'inflammatory' set, glycerides were the most common group ($n = 26$, 51%), followed by glycerophospholipids ($n = 14$, 27%), with the remaining ones comprising 4 AC, 4 amino acids, and 3 sphingolipids. The 26 metabolites that belonged to the 'inflammatory' set and not the 'tumorous' set comprised 18 glycerophospholipids (69%), 5 AC (19%), 2 amino acids, and creatinine. Among the lipid metabolites in the two unique sets, polar lipids (glycerophospholipids) were dominant in the 'inflammatory' set, whereas non-polar lipids (AC and glycerides) were dominant in the 'tumorous' set (Supplementary Fig. 3).

Next, we evaluated the overlap between the 'LM diagnostic' set and the 'tumorous' and 'inflammatory' sets. 40 out of 44 (91%) 'LM diagnostic' metabolites were common to both the 'tumorous' set and the 'inflammatory' set, with the four exceptions being CE(17:2), PC(41:5), PC-O(36:3), and AC(3:0), the last of which was shared by the 'tumorous' set (Fig. 5A). When we evaluated the diagnostic performance of these four metabolites unique to LM diagnostic in a logistic regression model, they discriminated LM from PBT achieving an AUC of 0.897 (Fig. 5D). Among the 40 metabolites in the 'LM diagnostic' set that were also in the 'tumorous' set and the 'inflammatory' set, 36 (90%) had higher levels in LM than in PBT, with the exceptions being AC(7:0), PC(40:7), PC(44:3), and Thr. In addition, the levels of all 40 of these shared metabolites in LM was between those in HC and ID/PBT. For example, the level of AC(4:O-OH) was lowest in ID/PBT, higher in LM, and highest in HC (HC > LM > ID/ PBT), whereas that of Thr was vice versa (ID/PBT > LM > HC).

Metabolites discriminating other clinical characteristics such as CSF sampling sites, intra-axial versus extra-axial brain tumors, and glial vs. non-glial malignant tumors

We explored the possibility that CSF metabolites could be used to differentiate additional clinical variables, including CSF sampling sites, metastasis patterns (leptomeningeal vs. parenchymal), tumor origins (metastatic vs. primary), benign extra-axial vs. malignant intra-axial

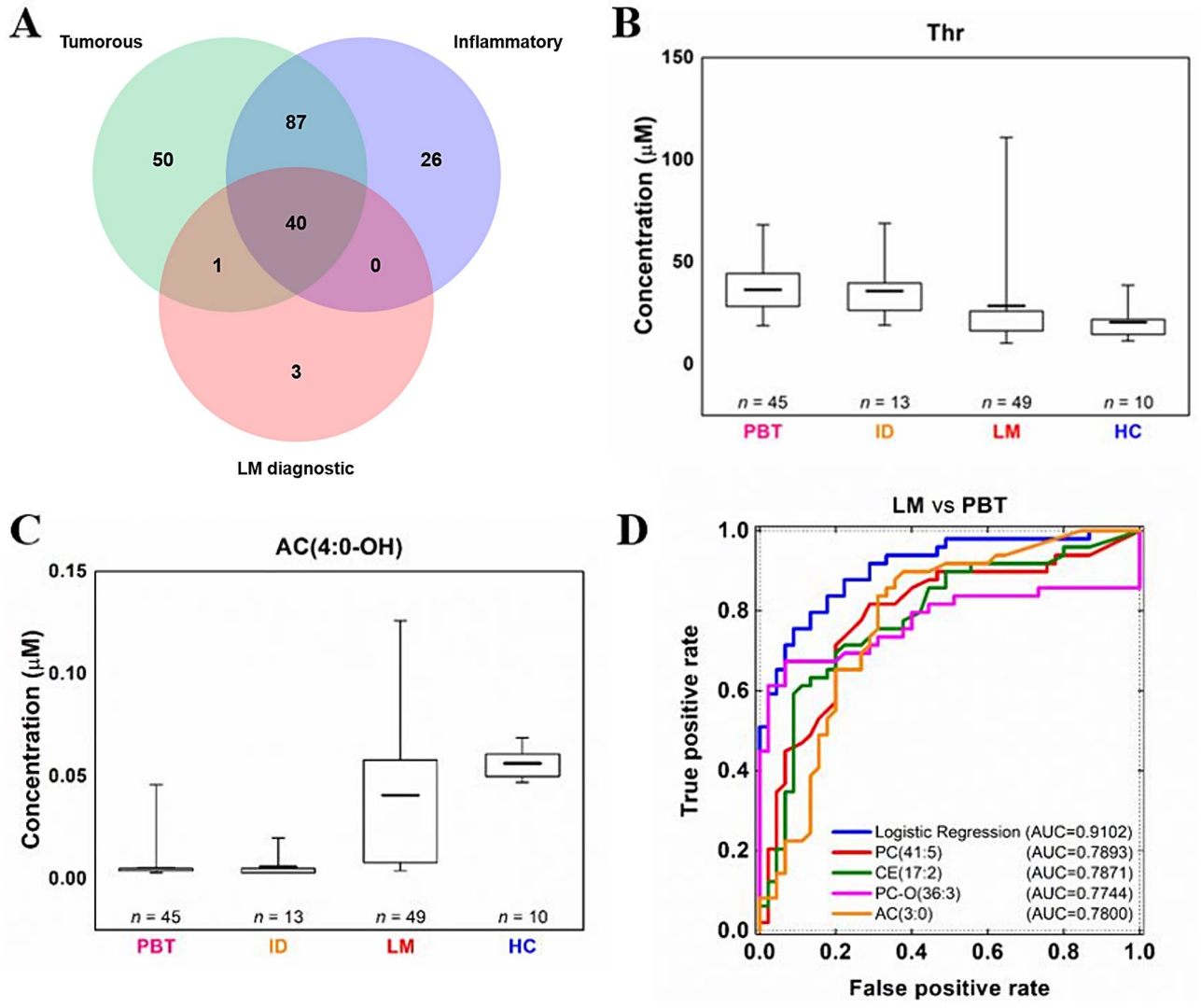

Fig. 5 Characteristics of discriminative metabolites for leptomeningeal metastasis, parenchymal brain tumor, and inflammatory disease. **A** Venn diagram of discriminative candidate metabolites between 'LM diagnostic' (LM vs. PBT) and 'tumorous' (PBT vs. HC) and 'inflammatory' (ID vs. HC) samples. **B-C** Box plots depicting levels of (**B**) threonine and (**C**) AC(4:0-OH) among patient groups. **D** Logistic regression model with three metabolites that were exclusive to the LM diagnostic profile. Notes: PBT, parenchymal brain metastasis; HC, healthy control; ID, inflammatory disease; LM, leptomeningeal metastasis; Thr, threonine

BT, and glial vs. non-glial malignant BT (Supplementary Table 9).

Sampling sites were evaluated within the LM group. 122 metabolites were discriminative between lumbar ($n=11$) and ventricular ($n=38$) sampling sites (AUC = 0.75 ~ 0.91). Among these, 99 (81%) had higher levels in samples taken from lumbar sites, whereas levels of 33 metabolites (19%) were higher in ventricular samples. A logistic regression model including the metabolites with the top 11 AUC values [Pro, AC(2:0), PC(34:4), Val, AC(0:0), PC-O(40:5), AC(7:0), PC(38:1), Gly, PC(34:3), and PC-O(34:1)] achieved 100% sensitivity and specificity.

We evaluated the ability of the metabolites in the LM ($n=49$) and BM ($n=15$) samples to discriminate between leptomeningeal and parenchymal metastases. 52 metabolites were discriminative (AUC = 0.75 ~ 0.93), and 42 (81%) of these had higher levels in LM than in BM, whereas the remaining 10 had higher levels in BM than in LM. A logistic regression model including the metabolites with the top 12 individual AUC values [AC(4:0-OH), AC(8:1), AC(8:0), AC(18:1-OH), AC(5:0), AC(11:0), AC(5:1), AC(6:0), AC(9:0), AC(7:0-DC), AC(6:0-OH), and PC(36:0)] reached an AUC of 1.0 overall.

Under the assumption that there might be differences in tumor microenvironments, we evaluated the ability of the metabolites in the BM ($n=15$) and BT ($n=30$)

samples to discriminate between metastatic and primary brain tumors. Only three metabolites—PC(32:5), PC(32:5), and AC(3:1)—were discriminative, with AUCs of 0.76 to 0.81. All showed higher levels in BM than in BT.

To identify metabolites that could discriminate according to tumor malignancy, we compared the levels of metabolites in samples from patients with benign extra-axial tumors ($n = 10$) and malignant intra-axial tumors ($n = 20$). We found 19 discriminative metabolites with individual AUCs of 0.76 to 0.86. Among these, 16 (84%) metabolites had higher levels in extra-axial benign BT samples than in intra-axial malignant BT samples. A logistic regression model including the metabolites with the top eight individual AUCs [PC(38:3), PC(38:7), TG(54:5), PC(38:6), PC(34:2), PC(40:9), creatinine, and AC(3:0-OH)] achieved 100% specificity and sensitivity.

To identify metabolites that could discriminate between malignant intra-axial tumors with different origins, we compared the levels of metabolites in samples from patients with gliomas ($n = 10$) and non-glial malignant BT ($n = 10$). We found 48 discriminative metabolites with individual AUCs of 0.76 to 0.90. Among these, 31 (65%) had higher levels in glioma samples than in non-glial malignancy samples. A logistic regression model including the metabolites with the top eight individual AUCs [(PC(36:3), PC(39:1), TG(50:4), PC(35:3), PC(37:3), PC-O(38:3), CE(16:0), and PC(33:5)] achieved 100% sensitivity and specificity.

Discussion

We investigated CSF metabolomics in LM using targeted MS to achieve quantitative comparative profiling with control groups including patients with other BT or BM. Although the number of CSF samples in this study is too small for our results to be conclusive, we were able to achieve diagnostic metabolic profiling with 100% sensitivity and 100% specificity.

The usefulness of MS-based CSF metabolomic profiling

Through both non-targeted and targeted metabolomics, previous studies showed that metabolomic profiles of cancer tissues or plasma could discriminate between patients with cancer and healthy controls and provide information about cancer pathogenesis [7, 22]. As CSF is in direct contact with the CNS, it can inherently reflect metabolic changes arising from CNS disease processes. For example, tau and amyloid β protein accumulation in neurons of Alzheimer's disease patients was better reflected in CSF than in serum, and the levels estimated from CSF correlated with disease progression [24, 25]. As advancements in MS resolution have made detectable LMIs in CSF plentiful enough to be analyzed, many studies using non-targeted MS with a relatively small number of samples have been able to set up discriminative profiles for different patient groups [19]. Dekker et al. investigated the use of MALDI-TOF MS-based profiling of trypsin-digested CSF peptides to discriminate between metastatic breast cancers with ($n = 54$) or without LM ($n = 52$) [26]. In their study, 164 out of 895 possible peak positions were discriminative with 79% sensitivity and 76% specificity for detecting LM; however, the accuracy was not superior to that of traditional diagnostic methods such as CSF cytology or gadolinium-enhanced MRI [16, 18]. In our previous study using non-targeted triple-TOF MS, we identified 1,440 differentially detected LMIs among 10,905 identifiable LMIs, and 21 selected LMIs were able to completely discriminate LM ($n = 67$) from BT ($n = 20$) and BM ($n = 9$). However, appropriate standard materials and protocols for the identification and quantification of LMIs were needed for validation studies.

Compared with non-targeted studies, targeted MS-based metabolomic studies have many advantages, including that (1) the identified metabolomic profile can unveil associated molecular changes, (2) quantitative measurements enable accurate comparisons of metabolite levels with standard materials, and (3) the use of a standard protocol can overcome batch effects from multiple measurements and enable multi-institutional data gathering [7, 27]. For these purposes, it is important to evaluate all metabolites related to the molecular pathway of interest together and to have an appropriate internal standard. In this regard, commercially available targeted MS kits, equipped with standardized protocols and internal standards, not only can be a useful diagnostic aid in clinical practice but also help us to gain insights into dysregulated metabolism of cancer cells and their interaction with the tumor microenvironment. While non-commercial, self-retrieved targeted MS studies typically detect a limited number of metabolites, commercially available kits offer standardized protocols that reduce measurement variability and continue to expand the range of measurable metabolites. With ongoing upgrades and advancements, these kits may eventually cover most metabolites within specific metabolic pathways. A study by Siskos et al. using the Absolute IDQ®-p180 kit (including 40 AC, 21 amino acids, 19 biogenic amines, 15 sphingolipids, and 90 glycerophospholipids) in human serum samples showed a median inter-laboratory coefficient of variation (CV) of 7.6%, with 85% of metabolites exhibiting a median inter-laboratory CV < 20% [27]. Another study evaluated CSF metabolites using the same p180 kit from Alzheimer's disease patients, and dichotomized patient groups according to amyloid β and tau levels showed that levels of a specific SM lipid metabolite (d18:1/18:0) were in accordance with disease progression [28]. In a later study, Carlsson et al. applied the upgraded

Absolute IDQ-p400® kit for CSF metabolomic analysis in healthy controls and multiple sclerosis patients, detecting 196 (48%) of 408 targeted metabolites above the limit of detection, with 35 absolutely quantified [20]. These studies highlight the potential for disease-specific profiling and the expanded coverage of commercially available targeted MS kits.

In the present study, we utilized the current Absolute IDQ-p400® targeted metabolomics kit in conjunction with high-resolution mass spectrometry (HRMS) to analyze CSF samples from HC, LM, PBT, and ID groups. As a result, we could successfully discriminate LM from PBT using a logistic regression model including 21 AC and PC lipid metabolites. Three lipid molecules that were not shared between the discriminatory metabolite sets for tumorous and inflammatory diseases could differentiate LM from PBT with an AUC of 0.90. Our results suggest the possibility of using CSF lipidomics as an aid to augment CSF cytology for patients with LM.

The possibility for CSF metabolomics to reflect CNS tumor activity or interaction with the tumor microenvironment

Almost all cancer cells, regardless of their type, reprogram their metabolism to enable neoplastic transformation, tumor progression, and therapy resistance [29, 30]. The dependency of cancer cells on inefficient anaerobic glycolysis, known as the Warburg effect, is an example of this metabolic reprogramming [21]. As a consequence of the Warburg effect, a huge amount of glucose is converted to NADPH in the pentose phosphate pathway, resulting in an over-reduced state of the mitochondrial matrix. Increased fatty acid β-oxidation and lipid synthesis can result from metabolic reprogramming in cancer cells, as many in vitro studies have reported dysregulated glucose and amino acid metabolism in cancer cells [21]. However, in clinical samples, especially in biofluids, it is difficult to evaluate exact differences or shifts of glycolysis or the Krebs cycle. The reasons for this include that (1) it is difficult to measure all related metabolites and intermediate byproducts together, (2) it is not practical to restrict all nutritional inputs to patients at the same level, and (3) steroids and intravenous supplements have confounding effects on the measurements. In the present study, we confirmed that hexose levels were affected by intravenous infusion or steroid use history, and amino acids and their metabolic intermediates failed to show significant differences between patients with CNS cancer and healthy controls.

Fatty acids with various lengths and degrees of desaturation are the main building blocks of lipid species that are abundant in the CNS, including DG, PC, and their byproducts such as phosphatidic acid, phosphatidylethanolamine, and phosphatidylserine, which can be involved in various metabolic pathways to accomplish key functions such as synaptogenesis and impulse conduction [29, 31]. Their structural diversity contributes to the composition of various biological membranes, cell signaling via secondary messengers, and energy storage [29]. In the context of metabolism, cancer cells rely on their ability to quench metabolic stress by increasing de novo biosynthesis and exogenous uptake of fatty acids to maintain rapid proliferation.

High PC levels have been consistently observed in tissues from various types of cancer, including breast [32], colorectal [33], and thyroid papillary [34] cancers and hepatocellular carcinoma [22], and increased cell membrane turnover in cancer cells was suggested to be an underlying mechanism. Furthermore, PC catabolism generates phosphatidic acid, diacylglycerol, LPC, and arachidonic acid, which have protumoral effects [35]. In the present study, PC levels were significantly increased in LM compared with those in PBT and HC, possibly as a result of neuronal/glial-cell membrane shedding, which is a natural consequence of floating cancer cells adhering to the CNS pial membrane. In the same context, levels of SM, which is enriched in CNS cell membranes as a byproduct of PC, were also increased in LM compared with those in the other groups.

LPC and PC derivatives, as byproducts of PC metabolism, are known to be consumed at elevated rates in cancer cells and may have a role in metastasis and immune reaction [35, 36]. Taylor et al. measured serum LPC along with nutritional and inflammatory parameters in 59 patients with cancer [37]. The LPC levels in the patients corresponded to the lower limit of those in healthy controls and were inversely correlated with the levels of plasma C-reactive protein and whole-blood hydrogen peroxides. Based on those findings, the authors suggested that LPC concentrations are associated with high metabolic activity and activated inflammatory processes. In the present study, LPC levels were significantly decreased in PBT compared with LM and HC. Although we did not directly measure choline kinase activity, we assume that these results were due to increased consumption of LPC by cancer cells, as PBT had the greatest mass of cancer cells among the three groups of comparison.

AC play a major role in regulating intracellular metabolism, serving as carriers to transport activated long-chain fatty acids into mitochondria for β-oxidation as a major source of energy for cell activities [38]. Elevated fatty acid oxidation in cancer cells contributes to rapid proliferation, phospholipid synthesis, and chemo-resistance [21, 30]. Studies of tissue and serum AC levels in patients with liver disease suggested that AC levels were proportional to disease progression in fatty liver disease, hepatitis B viral hepatitis, cirrhosis, and hepatocellular carcinoma [38, 39]. In accordance with different metabolic pathways in the mitochondria, elevated serum

levels of long-chain AC and decreased levels of medium and short-chain AC have been reported in cirrhosis and hepatocellular carcinoma [9, 40]. In our study, the levels of long-chain AC, but not short/medium-chain AC, were decreased in PBT compared with those in LM and HC. Although it is not conclusive from this exploratory study, decreased long-chain AC levels might result from inefficient AC shuttling between cytosol and mitochondria, as the calculated enzyme activity of both CPT1 and CPT2 was significantly lower in PBT than in HC.

Limitations of a commercial targeted MS metabolomics profiling in clinical practice

A primary limitation of the p400 kit is its inability to differentiate key monosaccharides and TCA cycle derivatives, measuring only hexoses; as a result, this study could not assess cancer-specific alterations in glycolysis or glucose metabolism. Accurate assessment of glucose metabolism in such studies would require strict control of intravenous fluid and steroid administration.

Additional limitations include the relatively small number of CSF samples in each group of comparison and the lack of a validation study for the selected discriminating metabolites. Validation was particularly challenging for lipid metabolites, given the variability in carboxyl chain lengths and saturation of each AC, PC, and SM variant, and their subclass interactions, which are not yet fully understood [41, 42]. Additionally, we had not initially balanced demographic profiles when selecting samples, focusing instead on ensuring sufficient number of samples of each CNS tumor type and disease of interest for comparison. Consequently, we did not perform statistical verification on these demographic profiles, as the sample sizes were too limited to provide robust statistical power. In the future studies, we should not only perform a validation study with a large number of samples but also prepare a case-control cohort study to minimize potential biases arising from demographic and clinical variables, such as nutritional and systemic cancer status, before advancing to clinical trial [37].

Another weakness of this study is that, unlike metabolites in tissues per se, metabolites in biofluids can come not only from cancer cells but also from normal cells composing the organs (e.g., brain parenchymal cells in CSF). Thus, the levels of tumor-originated metabolites are likely affected by the tumor burden, and it is practically impossible to control the tumor burden in intra-group or inter-group comparisons. Furthermore, as we did not analyze the corresponding serum levels of CSF metabolites, it is hard to exclude the influence of serum metabolites that cross the brain-CSF barrier [43], which is affected not by the CNS tumor status but by the systemic cancer status.

Despite these limitations, we believe that our CSF metabolomics profiles of patients with LM reflect the unique environment of floating cancer cells and the driver mutations allowing adaptation to an aqueous phase. Unlike the nutrient- and growth factor–enriched conditions which is relevant to solid tumor survival—a setting that has been extensively studied—LM presents a distinct environment requiring further investigation. To advance our understanding of this unknown unique pathogenesis, a multi-omics approach including genomics and proteomics of CSF from LM patients is needed, which we are currently developing as another project.

Conclusion

Using a commercial targeted MS metabolomics kit that measures 408 metabolites, we were able to quantify the levels of 201 metabolites in > 90% of CSF samples from healthy controls and patients with LM, parenchymal BT, or CNS inflammation. Most of the metabolites that were discriminative among different disease states were PC, LPC, or AC lipid metabolites, whereas amino acids, biogenic amines, and hexoses failed to show significant differences among patient groups and controls. These discriminative lipid metabolites warrants further investigation to determine their CNS distribution and quantification in different cell types.

A validation study of our discriminative metabolic CSF profiles should be performed with as many CSF samples as possible in a controlled cohort, and the kit should expand its coverage about glucose metabolism to enable us to differentially measure compounds from the Warburg effect, TCA cycle, pentose phosphate pathway and one carbon metabolism etc.

Abbreviations

CSF	Cerebrospinal fluid
CNS	Central nervous system
LMI	Low-mass ions
MS	Mass spectrometry
LM	Leptomeningeal metastasis
MRI	Magnetic resonance imaging
LC	MS-Liquid chromatography-mass spectrometry
LC	MS/MS-Liquid chromatography-tandem mass spectrometry
PCA	DA-Principal component analysis-based discriminant analysis
PBT	Parenchymal brain tumor
BM	Brain metastasis
BT	Primary brain tumor
HC	healthy control
HRMS	high-resolution mass spectrometry
TME	tumor microenvironment
ID	Inflammatory disease
PC	Phosphatidylcholines
AC	Acylcarnitines
TG	Triglycerides
SM	Sphingomyelins
LPC	Lysophosphatidylcholines
DG	Diglyerides
CE	Cholesteryl esters
Cer	Ceramides
FIA	Flow injection analysis
HESI	II-Heat electrospray ionization

PRM	Parallel reaction monitoring
HCA	Hierarchial clustering analysis
CPT1, 2	Carnitine palmitoyltransferase1, 2
CV	Coefficient of variation
IDH	Isocitrate dehydrogenase

Supplementary Information

The online version contains supplementary material available at https://doi.org/10.1186/s40170-024-00367-x.

Supplementary Material 1: Supplementary Fig. 1. Comparison of metabolic profiles between LM and NonLM groups. **A** Volcano plot with a fold change threshold of ±0.6 and a p-value threshold of 0.05. Labels indicate the top 10 metabolites based on p-value. **B** Principal component analysis plot showing a widely distributed LM cluster, with considerable overlap in the NonLM cluster

Supplementary Material 2: Supplementary Fig. 2. Metabolite levels according to each metabolite class among three groups with different tumor statuses (PBT, LM, and HC). **A** Amino acids. **B** Biogenic amines. Error bars represent the mean standard error

Supplementary Material 3: Supplementary Fig. 3. Calculated enzymatic activity of (**A**) Carnitine palmitoyltransferase 1 (CPT1) and (**B**) Carnitine palmitoyltransferase 2 (CPT2) among three groups with different tumor status (PBT, LM, and HC). Error bars represent the mean standard error. (*$0.01 < p < 0.05$; **$0.001 < p < 0.01$; *** $p < 0.001$)

Supplementary Material 4: Supplementary Fig. 4. Differential compositions of candidate discriminative metabolites in (**A**) the 'tumorous' set (PBT vs. HC), (**B**) the 'inflammatory' set (ID vs. HC), and (C) those common to both sets. Polar (ivory and orange) and non-polar (grey and blue) lipids were dominant in the 'tumorous' and 'inflammatory' sets, respectively

Supplementary Material 5: Supplementary Table 1. Demographic profiles of the study participants ($n = 117$)

Supplementary Material 6: Supplementary Table 2. Levels of 408 targeted metabolomes of all samples ($n = 117$)

Supplementary Material 7: Supplementary Table 3. Number of measured metabolite classes in CSF samples according to 10% intervals

Supplementary Material 8: Supplementary Table 4. CSF hexose level and use of dextrose-containing intravenous fluid and steroid

Supplementary Material 9: Supplementary Table 5. Comparison of metabolites in LM and HC samples

Supplementary Material 10: Supplementary Table 6. Comparison of metabolites in PBT, ID, and HC samples

Supplementary Material 11: Supplementary Table 7. Comparison of metabolites in LM and PBT samples

Supplementary Material 12: Supplementary Table 8. Comparison of discriminative candidate metabolites between 'LM diagnostic' (LM vs. PBT) and 'tumorous' (PBT vs. HC) and 'inflammatory' (ID vs. HC) samples

Supplementary Material 13: Supplementary Table 9. Comparison of other various characteristics between CSF

Acknowledgements
Not applicable.

Author contributions
HSG contributed to the conception and design of the work. KYL, JHK, JBP, BCY contributed to material preparation. KHK contributed to data acquisition, JHL contributed to data analysis and visualization, and all authors contributed to data interpretation. The first draft of the manuscript was written by HSG with contributions of all authors, and the manuscript was edited by SJ. All authors read and approved the final manuscript.

Funding
This research was funded by the National Cancer Center, Republic of Korea (NCC2410790-1), and a grant of the Korea Health Industry Development Institute, funded by the Ministry of Health and Welfare, Republic of Korea (HI17C1018).

Data availability
No datasets were generated or analysed during the current study.

Declarations

Ethics approval and consent to participate
This study followed the Helsinki declaration. All participants signed an informed consent form and this study was approved by the Institutional Review Board of our institute (Registration number: NCC2014-0135).

Consent for publication
All authors read and approved the final manuscript.

Competing interests
The authors declare no competing interests.

Author details
[1]Department of Neurosurgery, College of Medicine, Seoul National University, Seoul, Korea
[2]Department of Cancer Control, National Cancer Center Graduate School of Cancer Science and Policy, National Cancer Center, Goyang-si, Gyeonggi-do, Republic of Korea
[3]Biomarker Branch, and Cancer Diagnostics Branch, Division of Cancer Biology, Research Institute, National Cancer Center, Goyang-si, Gyeonggi-do, Republic of Korea
[4]Department of Cancer Biomedical Science, National Cancer Center Graduate School of Cancer Science and Policy, National Cancer Center, Goyang-si, Gyeonggi-do, Republic of Korea
[5]Neuro-oncology Clinic, National Cancer Center, Goyang-si, Gyeonggi-do, Republic of Korea
[6]InnoBation Bio, Seoul, Republic of Korea

Received: 8 September 2024 / Accepted: 11 December 2024
Published online: 21 January 2025

References

1. Debus OM, Lerchl A, Bothe HW, Bremer J, Fiedler B, Franssen M, Koehring J, Steils M, Kurlemann G. Spontaneous central melatonin secretion and resorption kinetics of exogenous melatonin: a ventricular CSF study. J Pineal Res. 2022;33:213–7.
2. Frankfort SV, Tulner LR, van Campen JP, Verbeek MM, Jansen RW, Beijnen JH. Amyloid beta protein and tau in cerebrospinal fluid and plasma as biomarkers for dementia: a review of recent literature. Curr Clin Pharmacol. 2008;3:123–31.
3. Romeo MJ, Espina V, Lowenthal M, Espina BH, Petricoin EF 3rd, Liotta LA. CSF proteome: a protein repository for potential biomarker identification. Expert Rev Proteom. 2005;2:57–70.
4. Diez B, Balmaceda C, Matsutani M, Weiner HL. Germ cell tumors of the CNS in children: recent advances in therapy. Childs Nerv Syst. 1999;15:578–85.
5. Nakagawa H, Kubo S, Murasawa A, Nakajima S, Nakajima Y, Izumoto S, Hayakawa T. Measurements of CSF biochemical tumor markers in patients with meningeal carcinomatosis and brain tumors. J Neurooncol. 1992;12:111–20.
6. Sasayama T, Nakamizo S, Nishihara M, Kawamura A, Tanaka H, Mizukawa K, Miyake S, Taniguchi M, Hosoda K, Kohmura E. Cerebrospinal fluid interleukin-10 is a potentially useful biomarker in immunocompetent primary central nervous system lymphoma (PCNSL). Neuro Oncol. 2012;14:368–80.
7. Beger RD, Dunn W, Schmidt MA, Gross SS, Kirwan JA, Cascante M, Brennan L, Wishart DS, Oresic M, Hankemeier T, Broadhurst DI, Lane AN, Suhre K, Kastenmuller G, Sumner SJ, Thiele I, Fiehn O. Kaddurah-Daouk R, for Precision M, Pharmacometabolomics Task Group-Metabolomics Society Initiative. Metabolomics enables precision medicine: A White Paper, Community Perspective. Metabolomics. 2016;12:149.

8. Lee JH, Kim KH, Park JW, Chang HJ, Kim BC, Kim SY, Kim KG, Lee ES, Kim DY, Oh JH, Yoo BC, Kim IH. Low-mass-ion discriminant equation: a new concept for colorectal cancer screening. Int J Cancer. 2014;134:1844–53.
9. Ballester LY, Lu G, Zorofchian S, Vantaku V, Putluri V, Yan Y, Arevalo O, Zhu P, Riascos RF, Sreekumar A, Esquenazi Y, Putluri N, Zhu JJ. Analysis of cerebrospinal fluid metabolites in patients with primary or metastatic central nervous system tumors. Acta Neuropathol Commun. 2018;6:85.
10. Nakamizo S, Sasayama T, Shinohara M, Irino Y, Nishiumi S, Nishihara M, Tanaka H, Tanaka K, Mizukawa K, Itoh T, Taniguchi M, Hosoda K, Yoshida M, Kohmura E. GC/MS-based metabolomic analysis of cerebrospinal fluid (CSF) from glioma patients. J Neurooncol. 2013;113:65–74.
11. Im JH, Yoo BC, Lee JH, Kim KH, Kim TH, Lee KY, Kim JH, Park JB, Kwon JW, Shin SH, Yoo H, Gwak HS. Comparative cerebrospinal fluid metabolites profiling in glioma patients to predict malignant transformation and leptomeningeal metastasis with a potential for preventive personalized medicine. EPMA J. 2020;11:469–84.
12. Liu Y, Hong Z, Tan G, Dong X, Yang G, Zhao L, Chen X, Zhu Z, Lou Z, Qian B, Zhang G, Chai Y. NMR and LC/MS-based global metabolomics to identify serum biomarkers differentiating hepatocellular carcinoma from liver cirrhosis. Int J Cancer. 2014;135:658–68.
13. Takahashi Y, Sakaguchi K, Horio H, Hiramatsu K, Moriya S, Takahashi K, Kawakita M. Urinary N1, N12-diacetylspermine is a non-invasive marker for the diagnosis and prognosis of non-small-cell lung cancer. Br J Cancer. 2015;113:1493–501.
14. Chamberlain MC. Leptomeningeal metastases: a review of evaluation and treatment. J Neurooncol. 1998;37:271–84.
15. Gwak HS, Lee SH, Park WS, Shin SH, Yoo H, Lee SH. Recent Advancements of Treatment for Leptomeningeal Carcinomatosis. J Korean Neurosurg Soc. 2015;58:1–8.
16. Freilich RJ, Krol G, DeAngelis LM. Neuroimaging and cerebrospinal fluid cytology in the diagnosis of leptomeningeal metastasis. Ann Neurol. 1995;38:51–7.
17. Glantz MJ, Cole BF, Glantz LK, Cobb J, Mills P, Lekos A, Walters BC, Recht LD. Cerebrospinal fluid cytology in patients with cancer: minimizing false-negative results. Cancer. 1998;82:733–9.
18. Straathof CS, de Bruin HG, Dippel DW, Vecht CJ. The diagnostic accuracy of magnetic resonance imaging and cerebrospinal fluid cytology in leptomeningeal metastasis. J Neurol. 1999;246:810–4.
19. Yoo BC, Lee JH, Kim KH, Lin W, Kim JH, Park JB, Park HJ, Shin SH, Yoo H, Kwon JW, Gwak HS. Cerebrospinal fluid metabolomic profiles can discriminate patients with leptomeningeal carcinomatosis from patients at high risk for leptomeningeal metastasis. Oncotarget. 2017;8:101203–14.
20. Carlsson H, Abujrais S, Herman S, Khoonsari PE, Akerfeldt T, Svenningsson A, Burman J, Kultima K. Targeted metabolomics of CSF in healthy individuals and patients with secondary progressive multiple sclerosis using high-resolution mass spectrometry. Metabolomics. 2020;16:26.
21. Zhelev Z, Aoki I, Lazarova D, Vlaykova T, Higashi T, Bakalova R. A Weird Mitochondrial Fatty Acid Oxidation as a Metabolic Secret of Cancer. Oxid Med Cell Longev. 2022;2022:2339584.
22. Wu T, Zheng X, Yang M, Zhao A, Li M, Chen T, Panee J, Jia W, Ji G. Serum lipid alterations identified in chronic hepatitis B, hepatitis B virus-associated cirrhosis and carcinoma patients. Sci Rep. 2017;7:42710.
23. Shim Y, Gwak HS, Kim S, Joo J, Shin SH, Yoo H. Retrospective Analysis of Cerebrospinal Fluid Profiles in 228 Patients with Leptomeningeal Carcinomatosis: Differences According to the Sampling Site, Symptoms, and Systemic Factors. J Korean Neurosurg Soc. 2016;59:570–6.
24. Byeon SK, Madugundu AK, Jain AP, Bhat FA, Jung JH, Renuse S, Darrow J, Bakker A, Albert M, Moghekar A, Pandey A. Cerebrospinal fluid lipidomics for biomarkers of Alzheimer's disease. Mol Omics. 2021;17:454–63.
25. Higginbotham L, Ping L, Dammer EB, Duong DM, Zhou M, Gearing M, Hurst C, Glass JD, Factor SA, Johnson ECB, Hajjar I, Lah JJ, Levey AI, Seyfried NT. Integrated proteomics reveals brain-based cerebrospinal fluid biomarkers in asymptomatic and symptomatic Alzheimer's disease. Sci Adv. 2020;6(43).
26. Dekker LJ, Boogerd W, Stockhammer G, Dalebout JC, Siccama I, Zheng P, Bonfrer JM, Verschuuren JJ, Jenster G, Verbeek MM, Luider TM, Smitt PA. MALDI-TOF mass spectrometry analysis of cerebrospinal fluid tryptic peptide profiles to diagnose leptomeningeal metastases in patients with breast cancer. Mol Cell Proteom. 2005;4:1341–9.
27. Siskos AP, Jain P, Romisch-Margl W, Bennett M, Achaintre D, Asad Y, Marney L, Richardson L, Koulman A, Griffin JL, Raynaud F, Scalbert A, Adamski J, Prehn C, Keun HC. Interlaboratory Reproducibility of a Targeted Metabolomics Platform for Analysis of Human Serum and Plasma. Anal Chem. 2017;89:656–65.
28. Locasale JW, Melman T, Song S, Yang X, Swanson KD, Cantley LC, Wong ET, Asara JM. Metabolomics of human cerebrospinal fluid identifies signatures of malignant glioma. Mol Cell Proteom. 2012;11(6):M111014688.
29. Koundouros N, Poulogiannis G. Reprogramming of fatty acid metabolism in cancer. Br J Cancer. 2020;122:4–22.
30. Li YJ, Fahrmann JF, Aftabizadeh M, Zhao Q, Tripathi SC, Zhang C, Yuan Y, Ann D, Hanash S, Yu H. Fatty acid oxidation protects cancer cells from apoptosis by increasing mitochondrial membrane lipids. Cell Rep. 2022;39:111044.
31. Cermenati G, Mitro N, Audano M, Melcangi RC, Crestani M, De Fabiani E, Caruso D. Lipids in the nervous system: from biochemistry and molecular biology to patho-physiology. Biochim Biophys Acta. 2015;1851:51–60.
32. Mori N, Wildes F, Kakkad S, Jacob D, Solaiyappan M, Glunde K, Bhujwalla ZM. Choline kinase-alpha protein and phosphatidylcholine but not phosphocholine are required for breast cancer cell survival. NMR Biomed. 2015;28:1697–706.
33. Kurabe N, Hayasaka T, Ogawa M, Masaki N, Ide Y, Waki M, Nakamura T, Kurachi K, Kahyo T, Shinmura K, Midorikawa Y, Sugiyama Y, Setou M, Sugimura H. Accumulated phosphatidylcholine (16:0/16:1) in human colorectal cancer; possible involvement of LPCAT4. Cancer Sci. 2013;104:1295–302.
34. Ishikawa S, Tateya I, Hayasaka T, Masaki N, Takizawa Y, Ohno S, Kojima T, Kitani Y, Kitamura M, Hirano S, Setou M, Ito J. Increased expression of phosphatidylcholine (16:0/18:1) and (16:0/18:2) in thyroid papillary cancer. PLoS ONE. 2012;7:e48873.
35. Saito RF, Andrade LNS, Bustos SO, Chammas R. Phosphatidylcholine-Derived Lipid Mediators: The Crosstalk Between Cancer Cells and Immune Cells. Front Immunol. 2022;13:768606.
36. Raynor A, Jantscheff P, Ross T, Schlesinger M, Wilde M, Haasis S, Dreckmann T, Bendas G, Massing U. Saturated and mono-unsaturated lysophosphatidylcholine metabolism in tumour cells: a potential therapeutic target for preventing metastases. Lipids Health Dis. 2015;14:69.
37. Taylor LA, Arends J, Hodina AK, Unger C, Massing U. Plasma lyso-phosphatidylcholine concentration is decreased in cancer patients with weight loss and activated inflammatory status. Lipids Health Dis. 2007;6:17.
38. Li S, Gao D, Jiang Y, Function. Detection and Alteration of Acylcarnitine Metabolism in Hepatocellular Carcinoma. Metabolites. 2019;9.
39. Zhou L, Wang Q, Yin P, Xing W, Wu Z, Chen S, Lu X, Zhang Y, Lin X, Xu G. Serum metabolomics reveals the deregulation of fatty acids metabolism in hepatocellular carcinoma and chronic liver diseases. Anal Bioanal Chem. 2012;403:203–13.
40. Lu Y, Li N, Gao L, Xu YJ, Huang C, Yu K, Ling Q, Cheng Q, Chen S, Zhu M, Fang J, Chen M, Ong CN. Acetylcarnitine Is a Candidate Diagnostic and Prognostic Biomarker of Hepatocellular Carcinoma. Cancer Res. 2016;76:2912–20.
41. Freysz L, Harth S, Dreyfus H. Topographic distribution of enzymes synthesizing phosphatidylcholine and phosphatidylethanolamine in chicken brain microsomes. J Neurochem. 1982;38:582–7.
42. Kulig W, Korolainen H, Zatorska M, Kwolek U, Wydro P, Kepczynski M, Rog T. Complex Behavior of Phosphatidylcholine-Phosphatidic Acid Bilayers and Monolayers: Effect of Acyl Chain Unsaturation. Langmuir. 2019;35:5944–56.
43. Borkowski K, Seyfried NT, Arnold M, Lah JJ, Levey AI, Hales CM, Dammer EB, Blach C, Louie G, Kaddurah-Daouk R, Newman JW. Integration of plasma and CSF metabolomics with CSF proteomic reveals novel associations between lipid mediators and central nervous system vascular and energy metabolism. Sci Rep. 2023;13:13752.

Publisher's note